

Energy-dependent anisotropic deformation of colloidal silica particles under MeV Au irradiation

T. van Dillen^{a)} and A. Polman

FOM-Institute for Atomic and Molecular Physics, Kruislaan 407, NL-1098 SJ Amsterdam, The Netherlands

W. Fukarek

Research Center Rossendorf, Institute of Ion Beam Physics and Materials Research, P.O. Box 510119, D-01314 Dresden, Germany

A. van Blaaderen

FOM-Institute for Atomic and Molecular Physics, Kruislaan 407, NL-1098 SJ Amsterdam and Debye Institute, Condensed Matter, Utrecht University, Princetonplein 5, NL-3584 CC Utrecht, The Netherlands

(Received 9 October 2000; accepted for publication 11 December 2000)

Spherical silica colloids with a diameter of $1.0\ \mu\text{m}$, made by wet chemical synthesis, were irradiated with 2–16 MeV Au ions at fluences in the range $(2-11)\times 10^{14}\ \text{cm}^{-2}$. The irradiation induces an anisotropic plastic deformation turning the spherical colloids into ellipsoidal oblates. After 16 MeV Au irradiation to a fluence of $11\times 10^{14}\ \text{cm}^{-2}$, a size aspect ratio of 5.0 was achieved. The size polydispersity ($\sim 3\%$) remains unaffected by the irradiation. The transverse diameter increases exponentially with ion fluence. By performing measurements as a function of ion energy at a fixed fluence, it is concluded that the transverse diameter increases linearly with the average electronic energy loss above a threshold value of $\sim 0.6\ \text{keV/nm}$. Nonellipsoidal colloids are observed in the case where the projected ion range is smaller than the colloid diameter. The data provide strong support for the thermal spike model of anisotropic deformation. © 2001 American Institute of Physics. [DOI: 10.1063/1.1345827]

MeV ion irradiation of amorphous materials such as metallic or silica glasses is known to cause anisotropic plastic deformation.¹⁻⁵ The result is an increase of the sample dimension perpendicular to the ion beam and a decrease in the direction parallel to the ion beam. This deformation process has been described mesoscopically by a viscoelastic model in which it is assumed that, due to the high electronic stopping power, a cylindrically shaped region around the ion track is subject to transient heating (thermal spike).⁶⁻⁸ During the thermal spike, shear stresses in the heated region relax, resulting in an associated shear strain that would freeze upon cooling of the thermal spike.

Experimentally, the anisotropic deformation has been studied by observing macroscopic dimensional changes of (metallic) glass foils^{1,2} or by studying the wafer curvature induced by irradiated thin films constrained on a substrate.^{4,5,9} Recently, we discovered that the deformation process also occurs in free-standing colloidal particles.¹⁰ Spherical colloidal SiO_2 and ZnS particles can be changed into ellipsoidal-shaped particles (oblates) due to a biaxial expansion perpendicular to the ion beam and a concomitant contraction along the ion beam. Colloidal particles with variable shape can find many applications in studies of self-assembly and phase behavior¹¹ and, except ion irradiation, no other methods exist that can produce nonspherical colloids that are monodisperse in size and shape. It is therefore important to study the dependence of the deformation effect on irradiation parameters such as ion energy and fluence.

In this letter, we study the dependence of the deformation of spherical silica particles on Au ion fluence and energy in the range 2–16 MeV. We find that the anisotropic deformation shows a gradual linear increase with electronic stopping power in the colloid, above a threshold of $\sim 0.6\ \text{keV/nm}$. We also study the special case in which the ion beam only partly penetrates the colloids, and find that nonellipsoidal particles are formed. This, together with the observed threshold, provides strong evidence for the thermal spike model for anisotropic deformation.

Colloidal silica spheres were made in a solution containing tetra-ethoxysilane, ammonia, and ethanol.¹² A drop of the colloidal dispersion was dried on a Si(100) substrate which had previously been cleaned for 10 min in a 1.0 M KOH–ethanol solution. Next, the particles were irradiated with Au ions using the 3 MV tandetron accelerator at the ion beam facility in Rossendorf.¹³ The ion beam was electrostatically scanned across a $5.1\times 5.1\ \text{cm}^2$ area. The ion energy was varied between 2 and 16 MeV and fluences ranged from 2 to $11\times 10^{14}\ \text{cm}^{-2}$. The ion beam energy flux was kept constant at a value of $0.16\ \text{W/cm}^2$ during all irradiations. The substrate holder was cooled with liquid nitrogen, and all irradiations were performed at an angle of 45° with respect to the Si surface. Vacuum grease at the backside of the sample was used to improve the heat contact between the sample and the cooled substrate holder. Note that the actual colloid temperature during irradiation might be higher than that of the holder. Ion ranges and electronic energy losses were calculated using TRIM98,¹⁴ a Monte Carlo calculation, using a silica structure with a density of $2.0\ \text{g/cm}^3$.¹⁵ Scanning electron microscopy (SEM) was performed at an energy of 10

^{a)}Author to whom correspondence should be addressed; electronic mail: dillen@amolf.nl

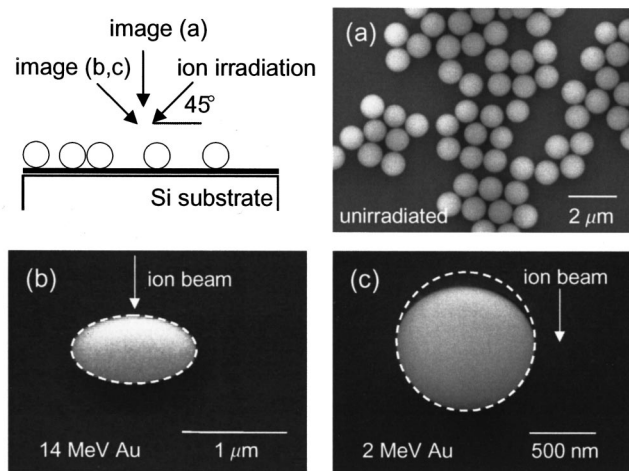


FIG. 1. Scanning electron microscopy (SEM) images of unirradiated and Au ion irradiated silica colloids on a silicon substrate. The ion beam direction and the different SEM viewing angles are depicted in the schematic. The arrows in the SEM images indicate the direction of the ion beam: (a) unirradiated silica colloids in top view; (b) deformed silica colloid after irradiation with 14 MeV Au⁴⁺ ions to a dose of $4 \times 10^{14} \text{ cm}^{-2}$ under 45° at 77 K; and (c) deformed silica colloid after a similar irradiation with 2 MeV Au²⁺ ions. Circular and ellipsoidal shapes are shown for reference by the dashed lines.

keV under different angles to image the particle shape before and after irradiation. Image processing and analysis software were used to characterize the particles before and after irradiation.

Figure 1(a) shows a SEM image of unirradiated silica particles on a silicon substrate viewed under normal incidence (see schematic in Fig. 1). The size distribution of 65 analyzed colloids is displayed in Fig. 2 (black histogram). The average colloid diameter is $1004 \pm 20 \text{ nm}$,¹⁶ with a standard deviation characterizing the size polydispersity $\sigma = 31 \pm 3 \text{ nm}$. This is typical for the colloid fabrication method used.¹²

Next, the colloids were irradiated with a 14 MeV Au⁴⁺ ion beam to a fluence of $4 \times 10^{14} \text{ cm}^{-2}$, under an angle of 45° (see schematic in Fig. 1). The projected ion range was calculated to be about 3.5 μm , well beyond the particle di-

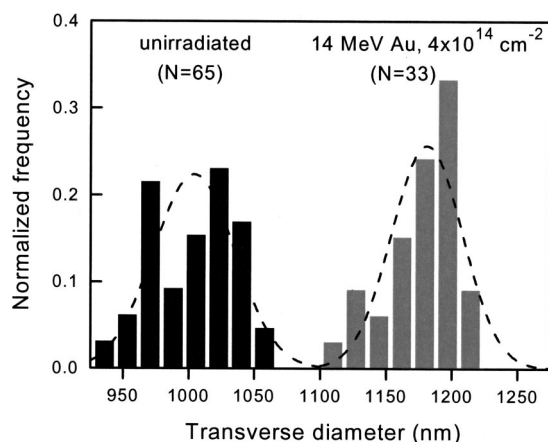


FIG. 2. Histogram of the transverse diameter size distribution of unirradiated silica colloids (black bars) and silica colloids irradiated with 14 MeV Au⁴⁺ ions to a fluence of $4 \times 10^{14} \text{ cm}^{-2}$ (gray bars). Gaussian distributions with standard deviations of $\sigma = 31 \text{ nm}$ (unirradiated) and $\sigma = 27 \text{ nm}$ (irradiated) are indicated by the dashed lines.

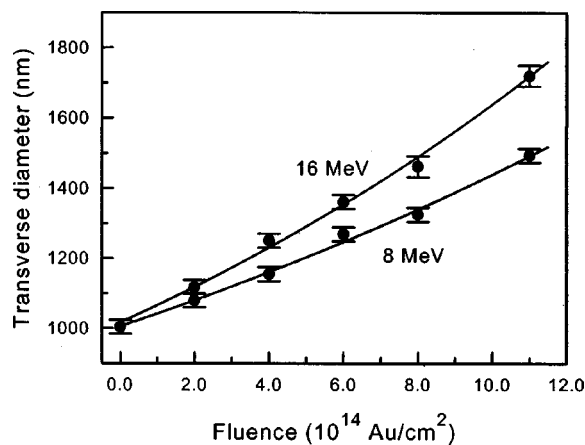


FIG. 3. Transverse diameter of the silica oblates as function of ion fluence. Results are shown for irradiations with 8 MeV Au³⁺ and 16 MeV Au⁵⁺. Exponential fits to the data are included.

ameter. Figure 1(b) shows a SEM micrograph after irradiation taken in the direction perpendicular to the ion beam. Clearly, the originally spherical particle has turned into an ellipsoidal oblate with a dimensional expansion perpendicular to the ion beam and a contraction parallel to the ion beam.

Figure 2 also shows the size distribution of the transverse diameter of 33 oblates after irradiation (gray histogram). This axis has increased to a mean value of $1181 \pm 20 \text{ nm}$, with $\sigma = 27 \pm 3 \text{ nm}$. This indicates that the ion irradiation process does not significantly increase the particle size polydispersity. Note that at a fluence of $4 \times 10^{14} \text{ cm}^{-2}$ each colloid has been impacted by some 10^7 ions. Any statistical variations are expected to be averaged out at this large number of ions. Assuming the colloidal volume remains constant after irradiation,¹⁰ the aspect ratio of the deformed colloids in Fig. 1(b) is calculated to be 1.63.

Figure 1(c) shows a SEM micrograph of a colloid after irradiation with 2 MeV Au²⁺ ions to a fluence of $4 \times 10^{14} \text{ cm}^{-2}$, viewed in the direction perpendicular to the ion beam. The projected range of 2 MeV Au ions in SiO₂ is about 0.55 μm , roughly equal to half the colloid diameter. This implies that the lower half of the colloid is not fully irradiated, except at the lateral side edges. Figure 1(c) clearly shows a nonellipsoidal shape of the colloid: the upper part of the colloid is deformed, whereas the lower part remains undeformed (see white dashed line). This clearly indicates that the deformation only takes place in the irradiated region of the colloid. From this we can conclude that the plastic deformation does not result from a uniaxial hydrostatic pressure generated by the ion beam, but results from single-ion impacts only. This is in agreement with the thermal spike model.

Figure 3 shows the transverse particle dimension after irradiation with 8 MeV Au³⁺ ions under 45° for fluences ranging from 2 to $11 \times 10^{14} \text{ cm}^{-2}$. The data were obtained from SEM micrographs taken in normal view. The transverse diameter increases with ion fluence from $1004 \pm 20 \text{ nm}$ for unirradiated particles to $1494 \pm 20 \text{ nm}$ after $11 \times 10^{14} \text{ cm}^{-2}$ irradiation. If the strain rate per ion, defined as $(1/L) \times dL/d\phi$ (L =transverse diameter, ϕ =fluence),¹ is constant with fluence, an exponential increase of the transverse diameter with ion fluence is expected. To describe the mea-

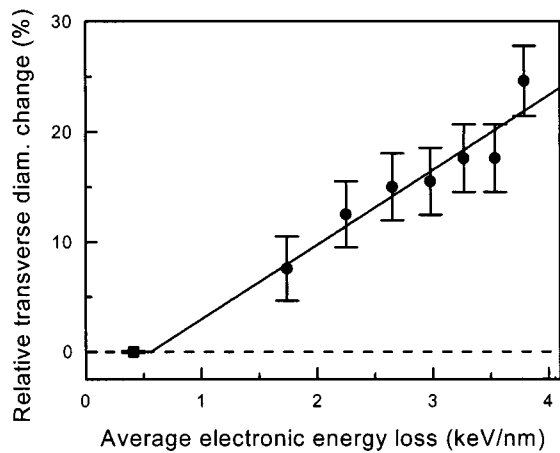


FIG. 4. Relative transverse diameter change of the silica oblates as a function of the average electronic energy loss at a fixed fluence of $4 \times 10^{14} \text{ cm}^{-2}$. Data were taken from experiments using ion energies in the range 4–16 MeV Au. The drawn line is a linear fit to the data. A data point for 500 keV Xe irradiation ($1 \times 10^{16} \text{ cm}^{-2}$) of 290 nm colloids for which no deformation was found is also indicated (solid square).

sured behavior, we fitted the data with an exponential function using a strain rate of $(3.6 \pm 0.1) \times 10^{-16} \text{ cm}^2/\text{ion}$.

Figure 3 also shows the fluence dependence for 16 MeV Au⁵⁺ irradiation. The colloid size aspect ratio after 16 MeV Au irradiation to a fluence of $11 \times 10^{14} \text{ cm}^{-2}$ is 5.0. Again, an exponential behavior, having a strain rate of $(4.8 \pm 0.2) \times 10^{-16} \text{ cm}^2/\text{ion}$, is observed in the same fluence range. Moreover, comparing the fluence dependence of the 8 and 16 MeV irradiations, it can be seen that at a fixed fluence the deformation increases with ion energy.

To investigate the energy dependence of the deformation, silica spheres were irradiated with Au ions at energies ranging from 4–16 MeV to a fixed fluence of $4 \times 10^{14} \text{ cm}^{-2}$. Figure 4 shows the measured relative change of the transverse diameter after irradiation, plotted as a function of the electronic stopping power in the colloid. The latter is calculated using a three-dimensional averaging method taking into account the changing shape of the colloid during irradiation. Also included in Fig. 4 is a data point obtained for 500 keV Xe irradiation of 290 nm silica colloids, for which no deformation is found (solid square), even for a fluence as high as $1 \times 10^{16} \text{ cm}^{-2}$.¹⁷

Figure 4 shows that the transverse diameter increases linearly with average electronic energy loss above a threshold value of $\sim 0.6 \text{ keV/nm}$. A threshold has also been found for the irradiation of silica foils, although larger in magnitude ($\sim 2 \text{ keV/nm}$).² The apparent threshold can be explained in terms of a transition from a more or less isotropically

shaped collision cascade for low energy irradiation, for which no anisotropic deformation occurs, to an anisotropically shaped thermal spike along the ion track at high energy.²

In conclusion, spherical colloidal silica particles undergo anisotropic plastic deformation under 2–16 MeV Au irradiation. The size polydispersity is not affected by irradiation. The size diameter increases exponentially with ion fluence at a rate that increases linearly with the average electronic energy loss in the colloid, above a threshold value of $\sim 0.6 \text{ keV/nm}$. Nonellipsoidal shapes are formed when the ion range is smaller than the colloid diameter. These data provide strong support for the thermal spike model for anisotropic deformation.

This work is part of the research program of the Foundation for Fundamental Research on Matter (FOM) and was financially supported by the Dutch Organization for Scientific Research (NWO). The authors gratefully acknowledge W. A. M. van Maurik and C. M. van Kats (Debye Institute, Utrecht University) for their support with the electron microscopy. This research was supported by the EC Large Scale Facility “AIM-Center for Application of Ion Beams in Materials Research,” Project No. ERB FMGE CT98 0146.

¹M.-d. Hou, S. Klaumünzer, and G. Schumacher, *Phys. Rev. B* **41**, 1144 (1990).

²A. Benyagoub, S. Löffler, M. Rammensee, S. Klaumünzer, and G. Saemann-Ischenko, *Nucl. Instrum. Methods Phys. Res. B* **65**, 228 (1992).

³S. Klaumünzer and A. Benyagoub, *Phys. Rev. B* **43**, 7502 (1991).

⁴E. Snoeks, A. Polman, and C. A. Volkert, *Appl. Phys. Lett.* **65**, 2487 (1994).

⁵M. L. Brongersma, E. Snoeks, T. van Dillen, and A. Polman, *J. Appl. Phys.* **88**, 59 (2000).

⁶H. Trinkaus and A. I. Ryazanov, *Phys. Rev. Lett.* **74**, 5072 (1995).

⁷H. Trinkaus, *Nucl. Instrum. Methods Phys. Res. B* **146**, 204 (1998).

⁸A. I. Ryazanov, A. E. Volkov, and S. Klaumünzer, *Phys. Rev. B* **51**, 12107 (1995).

⁹E. Snoeks, T. Weber, A. Cacciato, and A. Polman, *J. Appl. Phys.* **78**, 4723 (1995).

¹⁰E. Snoeks, A. van Blaaderen, T. van Dillen, C. M. van Kats, M. L. Brongersma, and A. Polman, *Adv. Mater.* **12**, 1511 (2000).

¹¹E. Snoeks, A. van Blaaderen, T. van Dillen, C. M. van Kats, K. Velikov, M. L. Brongersma, and A. Polman, *Nucl. Instrum. Methods Phys. Res. B* (in press).

¹²A. van Blaaderen and A. Vrij, *Langmuir* **8**, 2921 (1993).

¹³M. Friedrich, W. Bürger, D. Henke, and S. Turuc, *Nucl. Instrum. Methods Phys. Res. A* **382**, 357 (1996).

¹⁴J. F. Ziegler, J. P. Biersack, and U. Littmark, *The Stopping and Range of Ions in Solids* (Pergamon, New York, 1985).

¹⁵A. van Blaaderen and A. P. M. Kentgens, *J. Non-Cryst. Solids* **149**, 161 (1992).

¹⁶The error includes the error in the average determined from the size histogram and the pixel dimension in the digital SEM images.

¹⁷The error bar for this point in Fig. 4 ($\pm 0.1\%$) has been scaled to take into account the higher fluence.